IJECBE (2025), **3**, **2**, 283–299
Received (8 May 2025) / Revised (18 June 2025)
Accepted (19 June 2025) / Published (30 June 2025)
https://doi.org/10.62146/ijecbe.v3i2.122
https://ijecbe.ui.ac.id
ISSN 3026-5258

International Journal of Electrical, Computer and Biomedical Engineering

RESEARCH ARTICLE

Lightning Performance Design Review of 150kV Overhead Transmission Line

Fakhri Hakim*, Ismi Rosyiana Fitri, and Aji Nur Widyanto

Department of Electrical Engineering, Faculty of Engineering, Universitas Indonesia, Depok, Indonesia
*Corresponding author. Email: fakhri.hakim@ui.ac.id

Abstract

Lightning overvoltage constitutes the predominant cause of transmission line interruptions in Indonesia, significantly compromising system safety and reliability. This paper presents comprehensive simulations of lightning performance on 150kV overhead transmission lines using ATP-EMTP software, with particular focus on evaluating shielding failure and back flashover occurrences on one of the standard tower designs used by PT PLN (Persero). The transmission line model incorporates shielding wires, phase conductors, tower surge impedance, current-dependent footing resistance behavior, and arcing horns. Simulations were conducted to investigate three key aspects: maximum shielding failure current based on various Electrogeometric Model (EGM) constants, the impact of footing resistance on critical flashover current, and the effect of arcing horn length variations on critical flashover current. The analysis also accounts for phase angle variations in system voltage. Results highlight the significant influence of these variables on the Lightning Flashover Rate (LFR) of existing tower designs. Increasing footing resistance from 10Ω to 20Ω elevates Back Flashover Rate (BFOR) by 8.24%, while further increases to 30Ω and 40Ω yield only marginal increases of 8.71% and 8.93%, respectively. Notably, arcing horn gap length modifications demonstrate substantial performance improvements, with 1.4m and 1.5m gaps reducing LFR by 17.37% and 30.87%, respectively, compared to the 1.3m reference configuration. Analysis of maximum shielding-failure currents across varying EGM coefficient sets indicates that shield wires fail to intercept currents in the range of 2.53 kA to 52.81 kA.

Keywords: lightning surges, shielding failure, backflashover, overhead transmission lines, ATP-EMTP

1. Introduction

Owing to its equatorial maritime setting, Indonesia is subject to an exceptionally high incidence of lightning discharges [1]. Lightning induced outages rank among the primary causes of transmission line interruptions. Reducing their incidence demands a rigorous understanding of the underlying mechanisms and their simulation with appropriately detailed models, to avoid under or over estimation [2]. A lightning stroke to a shield wire or tower can drive the tower voltage sharply upward, triggering a backflashover and the accompanying short circuit fault. The backflashover manifests as an arc across the insulator string or arcing horn of one or more phases when the rapidly rising tower voltage momentarily exceeds the phase conductor voltage [3]. Low amplitude lightning strokes may bypass the overhead shield wires and terminate directly on a phase conductor, such strikes generally do not precipitate an insulator or arcing horn flashover. In practice, transmission line shielding is engineered based on an economically acceptable shielding failure rate. Consequently, only strokes whose peak currents fall within a specific intermediate range large enough to puncture the insulator or arcing horn air gap yet small enough to evade interception pose a credible flashover risk [4]. PT PLN (Persero) is a state-owned electricity company in Indonesia, one of whose businesses is as a transmission asset operator and owner. PT PLN (Persero) itself has transmission systems of 70kV, 150kV, and 500kV. However, the 150kV transmission network is generally used. Therefore, this research will focus on 150kV towers.

Numerous investigations have been undertaken to quantify and model the lightning performance of overhead transmission line. [2] examines the critical impact of transmission line modeling on understanding lightning overvoltage and the resulting backflashover phenomenon in power systems. The paper compare traditional, simplified models like J. Marti with Carson's formulation against more physically consistent models that account for factors such as displacement current, ground admittance correction, rigorous voltage definitions, and frequency-dependent soil parameters. [3] comprehensively surveys various models developed over decades for analyzing the transient behavior of high-voltage (HV) transmission line towers when struck by lightning. The paper categorize these tower models into four main types: lossless uniform transmission line (TL) models, multiconductor TL models, multistory models, and non-uniform TL models. [4] conduct details research into lightning attachment models and their application to transmission line shielding analysis. It introduces general formulas for calculating the maximum shielding failure current (IMSF) of overhead transmission lines, an essential parameter for insulation coordination studies and estimating shielding failure flashover rates. The paper compares various lightning attachment models, including electrogeometric, generic, Eriksson's, and statistical models, highlighting how different models yield varying IMSF values. [5] provides an in-depth analysis of lightning overvoltage on 132kV overhead transmission lines in Malaysia, a significant cause of power interruptions. The paper modeled these lines using ATP-EMTP software to investigate shielding failure patterns. The study details various components of the transmission line model, including wires, towers, and insulator strings, and how different lightning-strike current magnitudes impact induced voltages and flashover occurrences. [6] evaluates the necessity of surge arresters in overhead transmission lines by simulating backflashover incidents on a 132kV line using Electromagnetic Transient Program (PSCAD) software. It outlines the modeling of various transmission line components, including insulators, towers, and surge arresters, to investigate how different arrester placements affect backflashover rates. The research determines the optimal positioning for surge arresters to enhance lightning performance and reduce equipment failure, ultimately providing guidelines for transmission line designers.

Compared to previous papers, which have not provided an in-depth evaluation of 150kV transmission tower design, the most prevalent type owned by PT PLN (Persero), this study addresses this gap. PT PLN (Persero) is Indonesia's state-owned electricity company, serving as both a transmission asset operator and owner, with systems operating at 70kV, 150kV, and 500kV. This paper specifically evaluates 150kV transmission tower designs across a wide range of EGM constants to determine the phase-specific shielding failure maximum current. Furthermore, it quantifies the impact of arcing horn gap length, tower grounding resistance, and system voltage phase angle on the Backflashover Rate (BFOR), Shielding Failure Flashover Rate (SFFOR), and the aggregate Lightning Flashover Rate (LFR).

2. Research Methods

2.1 Methodology

An initial review was carried out to survey existing studies on overhead transmission line performance, incorporating PLN design standards and the typical specifications employed by PT PLN (Persero). Maximum shielding failure currents were then computed using the EGM across a range of published constant values. Subsequently, ATP-EMTP simulations were performed with the selected components, models, and parameters (detailed below). The primary simulation phase determined the critical current thresholds for both backflashover and shielding failure flashover under reference conditions, from which the SFFOR and BFOR were obtained. For advanced analysis, a sensitivity study examined the impact of variations in tower footing resistance and arcing horn gap on the critical currents, SFFOR, and BFOR. The research methodology flow chart is shown in Figure 1.

2.2 Transmission Line and Tower Specification

A lattice type structure, the predominant transmission tower configuration in the PT PLN (Persero) network is adopted as the study case. The transmission line and tower parameters are summarized in

Figure2 and Table 1. Based on PLN standard, 150 kV towers fitted with 12 disc of insulator strings shall employ an arcing-horn gap in the 1.3 m—1.5 m range. Although PLN specifies 10 Ω as the tower footing resistance standard, this value is not always attainable in practice. Consequently, it is essential to quantify how deviations from that standard impact the BFOR.

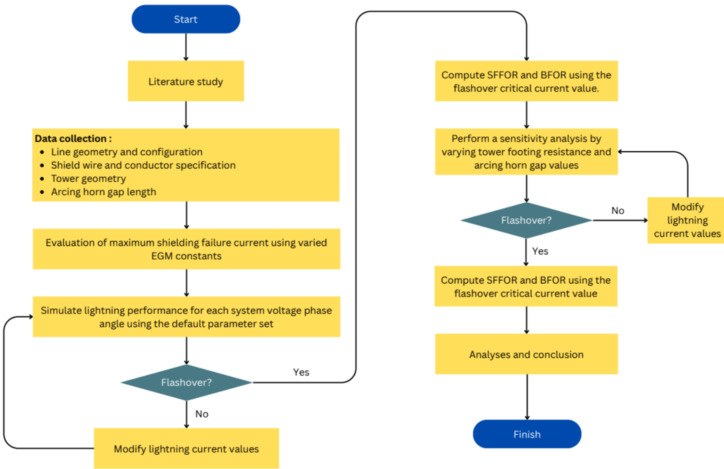

Figure 1. Flowchart of the Research Methodology

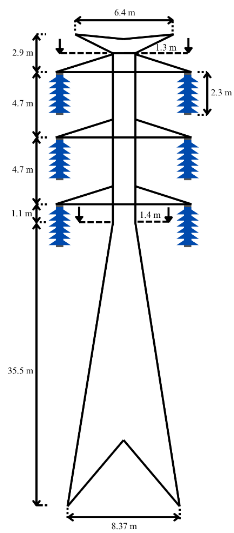

Figure 2. Transmission Tower Under Study

2.3 Modelling for Backflashover and Shielding Failure Flashover Analysis

2.3.1 Lightning Model

The lightning discharge is represented by a negative polarity CIGRE concave current, as illustrated by black line in Figure 3.

Front time, t_f is the time interval between the instant of the maximum peak and the intersection with the horizontal axis of the line crossing the 30% and 90% of the peak current represented by blue line or 'a-b line'.

Table 1. Transmission Line Spesification

Description	Details
System Voltage	150 kV
Conductor	1 x ACSR Zebra 400 mm^2
Earth Wire	OPGW 75 mm^2
Arcing horn gap	1.3 m (reference), 1.4 m, 1.5 m
Conductor DC Resistance	0.0674 Ω/km
Earth Wire DC Resistance	0.8 Ω/km
Footing Resistance	10 Ω (reference), 20 Ω, 30 Ω, 40 Ω
Soil Resistivity	100 Ω-m

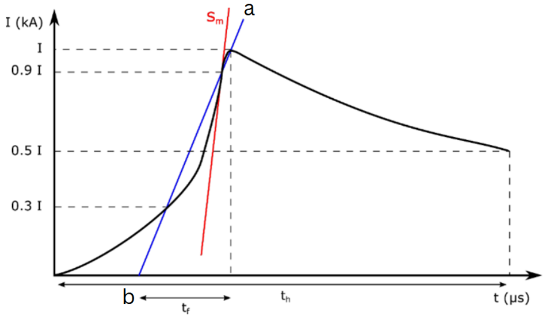

Figure 3. CIGRE Negative Polarity Lightning Concave Shape [7]

After the initial concave front and the abrupt rise, a point of maximum steepness (i.e. maximum rate of rise of the current) is reached and is specified in kA/µs. It is graphically represented by red line or 'S_m line'.

In the adopted model, waveform steepness scales linearly with the peak current, whereas the front time and half value time are held at their median values reported in [8], 3.83 µs and 77.5 µs, respectively.

The lightning channel is represented by a 400 Ω shunt resistance across the current source. These values are drawn from multiple literature sources. For example, [9] recommends a lightning path impedance between 400 Ω and 1000 Ω.

2.3.2 Transmission Tower

The tower is represented as a multistory, non uniform impedance structure [10], by divided the structure into multiple segments. The surge impedance of each segment is derived from its height and mean equivalent radius. The crossarm effect is represented by inserting parallel R–L branches between adjacent tower segments.

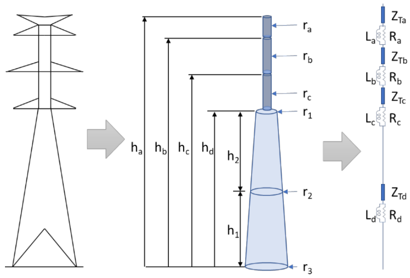

Figure 4. Transmission Tower and Equivalent Circuit [11]

Following the procedure of [11], the surge impedances of the upper segments, Z_{Ta} - Z_{Tc} are determined using the calculation method presented in [12]:

$$Z_T = 60cosh^{-1}(\frac{h}{r}) \tag{1}$$

where r (m) denotes the conductor section radius, h (m) is the non zero height above the ground. Accordingly, the surge impedance at the tower base, Z_{Td} can be evaluated using the following equation [13]:

$$Z_T = 60\left\{ln\left[cot\frac{\theta}{2}\right]\right\} \tag{2}$$

$$\theta = tan^{-1}\left(\frac{r_{av}}{H_t}\right) \tag{3}$$

$$r_{av} = \frac{r_1h_2 + r_2h_t + r_3h_1}{H_t} \tag{4}$$

where r_{av} (m) represents the section's mean equivalent radius, H_t (m) is the sum of h_1 and h_2, representing the section's overall height. The presented surge impedance formulations are valid only for cylindrical conductor geometries. In the case of box type cross section structures (e.g., conventional lattice towers), determine the equivalent radius using [11]:

$$r_{eq} = \frac{a + b}{\pi} \tag{5}$$

where a (m) is the section width and b (m) its depth. The resistor values are then computed as [14]:

$$r_i = \Delta R_i.l_i \tag{6}$$

regarding the tower's base resistor:

$$\Delta R_d = \frac{2.Z_{rd}}{h_d}in(\frac{1}{\alpha_d}) \tag{7}$$

with respect to the resistors of the upper segments:

$$\Delta R_i = \frac{2.Z_{ri}}{(h_a - h_d)} in(\frac{1}{\alpha_i}) \tag{8}$$

in which l_i (m) specifies the length of section i (from points 'α' to 'd'). Z_{Ti} (Ω) its corresponding surge impedance, and α the attenuation constant set to 0.89 for all segments. Inductor values for each tower section are evaluated using the equations below [14]:

$$L_i = 2\tau R_i \tag{9}$$

$$\tau = \frac{H_a}{c} \tag{10}$$

where c (m/s) representing the speed of light, 3 x 10^{-8}.

2.3.3 Overhead Transmission Lines

ATP/EMTP offers a suite of line models, such as Bergeron, Pi, J.Marti, Noda, and Semlyen. The model used in this paper is J. Marti [15], because the wire distribution parameters of Jmarti model are related to the uneven distribution characteristics of lightning current frequency and wave impedance[16]. This model includes the frequency dependence of the line parameter, their distributed nature and assumes a real and constant transformation matrix to decouple the propagation modes. The line model has been very reliable and accurate for most of the overhead line cases [17], besides being a commonly used model to represent transmission networks and tower conductors [5]. Furthermore, a study by [18] investigated a new method considering the influence of the soil and frequency effects to evaluate atmospheric overvoltages in overhead transmission lines. The results obtained from this method showed a closer agreement with the J. Marti model compared to the Bergeron model.The parameters such as conductor radius and conductor position from Figure 2 and Table 1 are utilized as variables for the line model parameters to represent the existing transmission system.

2.3.4 Arcing Horn Flash Model

The breakdown characteristics and underlying physical processes of the discharge mechanism are examined using the leader progression model, in which streamers initiate along the arcing horn once the applied voltage exceeds the corona inception threshold and, if sustained, evolve into a leader channel. Flashover occurs when this leader bridges the horn gap, and the total flashover time is given by the following equation [8]:

$$t_c = t_i + t_s + t_l \tag{11}$$

where t_i (μs) represents the corona inception time, t_s (μs) is the time streamers need to bridge the gap, and t_l (μs) is the leader propagation time.

In this work, the CIGRE leader development model [8] was implemented via the ISF MODELS language, as detailed in [19]. A streamer is deemed fully developed when it satisfies the following equation [8]:

$$U(t_s) = E_0 d \tag{12}$$

in this expression, E_0 (kV/m) denotes the critical inception stress across the gap (670 for negative polarity), d (m) the horn-gap length, and the leader propagation speed follows the definition in [8]:

$$\frac{dl}{dt} = k_1 U(t) \left[\frac{U(t)}{x} - E_0 \right] \tag{13}$$

in which, k_1 ($m^2/V^2/s$) denotes the negative-polarity air gap parameter (1.0×10^{-6}), x (m) represents the unbridged portion of the arcing-horn gap.

2.3.5 Tower Footing Resistance

As defined in [8], the tower footing resistance is modeled as a current dependent function, incorporating soil ionization effects, given by:

$$R(I) = \frac{R_0}{\sqrt{1 + \frac{I}{I_g}}} \tag{14}$$

where R_0 (Ω) is the footing resistance at low current and frequency, I (kA) the applied current and I_g (kA) the critical current for initiating soil ionization, given by:

$$I_g = \frac{E_0 \rho}{2\pi R_0^2} \tag{15}$$

with ρ (Ωm) represents soil resistivity, E_0 (kV/m) is the critical ionization gradient of the soil, typically assumed to be 400 kV/m [11].

2.3.6 Backflashover Analysis

Effective shielding by ground wires can nonetheless produce indirect strikes to phase conductors. When a lightning impulse hits the shield wire or tower, the resulting leader may bridge the arcing horn gap and initiate a backflashover. The annual BFOR, normalized per 100 km of line, is given by [8]:

$$BFOR = 0.6 N_L P(I_c) \tag{16}$$

in this study, accounting for the power frequency voltage phase angle variation, the annual BFOR is calculated as [11]:

$$BFOR = 0.6 N_L \left\{ \sum_{\theta=0}^{2\pi} \frac{\Delta\theta}{2\pi} P\left[I_c(\theta) \right] \right\} \tag{17}$$

where $P(I_c)$ denotes the probability that the lightning current exceeds the critical threshold I_c (kA), evaluated by simulating currents from 0 to 335 kA, the maximum recorded negative polarity stroke in Indonesia [20], $\Delta\theta$ (°) is the phase angle increment, for which six representative angles are employed in this study, based on recommendation from [11] to reduce computational time, and N_L is the annual number of flashes intercepted by the shield wire, given by:

$$N_L = \frac{N_g}{10}(28h^{0.6} + b) \tag{18}$$

where N_g (strikes/km^2/year) denotes the regional ground flash density, taken as 3.2 strikes/km^2/year, the mean value observed on Java Island over the study period [1], h (m) is the tower height, b (m) is the distance between shield wires.

According to IEEE Std 1243-1997, the cumulative distribution function of lightning peak currents, *P(I)* is rigorously defined as [21].

$$P(I) = \frac{1}{1 + (\frac{I}{31})^{2.6}} \tag{19}$$

where I (kA) denotes the lightning current.

2.3.7 Shielding Failure Analysis

Electrogeometric models (EGMs) have been extensively employed in transmission line shielding design to protect phase conductors from direct lightning strikes and continue to underpin modern engineering practice [21]. The standard EGM schematic for the shield-wire arrangements is presented in Figure 5.

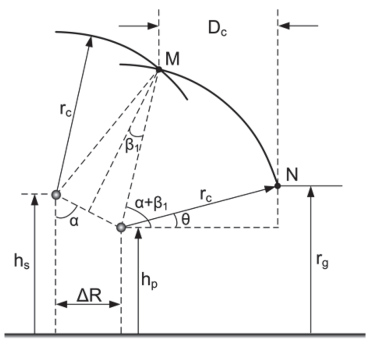

Figure 5. Shielding Analysis Based on the Electrogeometric Model (EGM) [22]

The maximum shielding failure current amplitude, I_{msf} (kA), is estimated as [4]:

$$I_{msf} = \left[\frac{\frac{\gamma(h_s+h_p)}{2}}{A(1-\gamma sina)}\right]^{\frac{1}{B}} \tag{20}$$

in which h_s (m) is the shield wire height, h_p (m) specify the vertical positions of the ground wire and phase conductor, α is the defined shielding angle, with constants A, B, and γ taking values of 8, 0.65 and 1, respectively, following Mousa and Srivastava [23]. These values serve as the reference/default since they approximate the median across all model variations. The maximum shielding failure current, I_{msf} (kA) will be calculated for each phase using varying sets of *A, B,* and γ constants summarized in Table 2.

Table 2. EGM Constant Values Derived from Multiple Model Variants [22]

Model	A	B	γ
Wagner et al. [24]	14.2	0.42	1
Young et al. [25]	27	0.32	1 for h<18m 444/(462-h) for h>18m h: shield wire height
Armstrong & Whitehead [26]	6.72	0.8	1.11
Brown & Whitehead [27]	7.1	0.75	1.11
E.R. Love [28]	10	0.65	1
E.R. Whitehead [29]	9.4	0.67	1
Suzuki et al. [30]	3.3	0.78	1
J. G. Anderson [31]	8	0.65	1/0.64 for UHV lines 1/0.8 for EHV lines 1 for other lines
Mousa & Srivastava [23]	8	0.65	1
IEEE Std [21]	10	0.65	1/[0.36+0.17ln(43-h)], for h<40m, 1/0.55 for h >40m h: phase conductor height

The resulting exposure width D_c (m), is then given by [32]:

$$D_c = \begin{cases} AI^B\left[cos\theta - cos(\alpha+\beta)\right] for\ I > (\frac{\gamma h_c}{A})^{1/B} \\ AI^B\left[1 - cos(\alpha+\beta)\right] for\ I \leq (\frac{\gamma h_c}{A})^{1/B} \end{cases} \tag{21}$$

$$\alpha = tan^{-1}\Delta R/(h_s - h_p) \tag{22}$$

$$\theta = sin^{-1}(\frac{1}{\gamma} - \frac{h_p}{AI^B}) \tag{23}$$

$$\beta = sin^{-1}\frac{\sqrt{\Delta R^2 + (h_s - h_p)^2}}{2AI^B} \tag{24}$$

SFFOR, expressed in flashovers per 100 km of line per year for each phase, quantifies the incidence of insulator flashovers resulting from shield wire interception failures and is computed as follows [11]:

$$SFFOR = \frac{N_g l}{1000}\int_{I=I_c}^{I=I_{msf}} D_c(I)f(I)dl \tag{25}$$

cccounting for the power frequency voltage phase angle variation, the equation become [11]:

$$SFFOR = \frac{N_g l}{1000}\sum_{\theta=0}^{2\pi}\left[\frac{\Delta\theta}{2\pi}\int_{I=I_c}^{I=I_{msf}} D_c(I,\theta)f(I)dl\right] \tag{26}$$

where I_c (kA) marks the current threshold for probable flashover occurrence, $f(I)$ corresponds to the probability density function of peak lightning-current magnitudes, calculated by:

$$f(I) = \frac{1}{\sqrt{2\pi\beta I}} exp(-\frac{z^2}{2}) \tag{27}$$

3. Results and Discussion

3.0.1 Maximum Shielding Failure Current

The maximum shielding-failure current for each phase of the studied tower was evaluated using the EGM with empirical constants A, B and γ drawn from multiple sources as presented in Table 2. Figure 6 represents the resulting maximum shielding failure currents that the ground wire may not intercept for each phase.

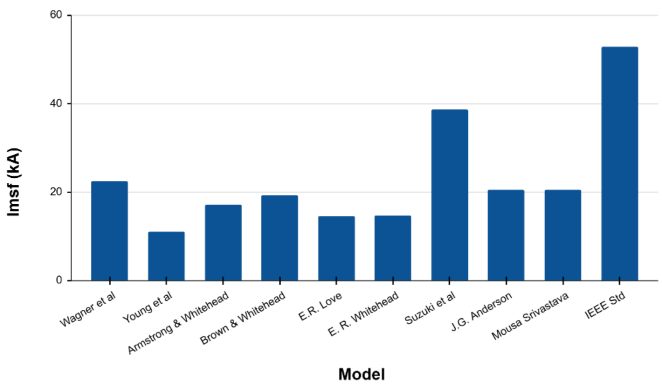

(a) Upper Phase

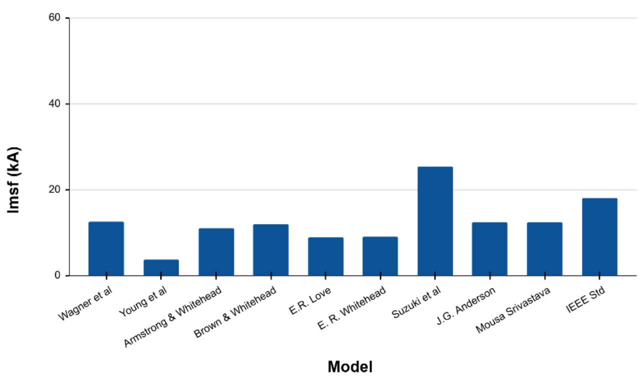

(b) Middle Phase

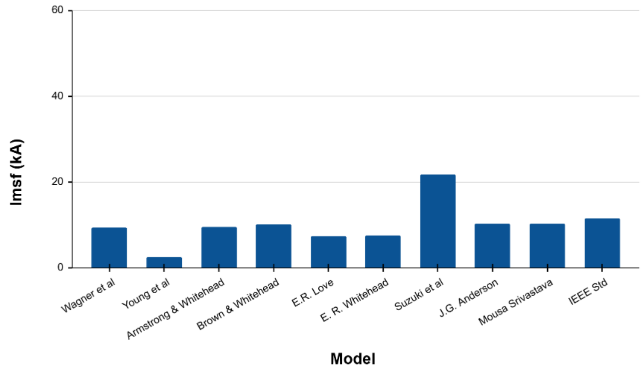

(c) Lower Phase

Figure 6. Variation of Maximum Shielding Failure Current for Each Phase Across Different Electrogeometric Model Constant Sets

Different EGM constant sets yield substantial variability in the maximum shielding-failure current for each phase. Specifically, the upper phase exhibits a range of 10.96 kA to 52.81 kA (median = 19.86 kA), the middle phase ranges from 3.74 kA to 25.39 kA (median = 12.20 kA), and the lower phase from 2.53 kA to 21.65 kA (median = 9.79 kA). The parameter values from Mousa and Srivastava are selected as the reference for this investigation, as they most closely approximate the median shielding failure currents across all phases.

3.0.2 Effect of Tower Footing Resistance Variation

An increase in tower footing resistance generally elevates the critical current required to initiate backflashover. However, the adopted current dependent footing resistance model yields a nonlinear relationship between footing resistance and critical current, I_c (kA). The simulated values for varying footing resistance levels are summarized in Table 3.

Table 3. Critical Current as a Function of Phase Angle and Tower Footing Resistance

I_c (kA) / Footing Resistance (Ω)	Phase Angle (°)					
	0	60	120	180	240	300
10	174.4	126.2	109.4	101	109.4	126.3
20	133.7	125.2	108.4	100	108.4	125.2
30	133.5	125	108.2	99.8	108.2	125
40	133.4	124.9	108.1	99.7	108.1	125

Next, the expected backflashover rate (BFOR) is evaluated, as illustrated in Figure 7.

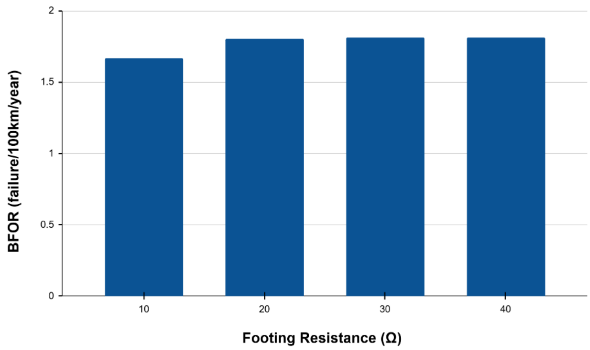

Figure 7. Backflashover rate (BFOR) as a Function of Tower Footing Resistance

From Table 3 and Figure 7, it is evident that the critical current, I_c (kA) and the BFOR exhibit a marked increase when the tower footing resistance rises from 10 Ω to 20 Ω, whereas for resistances between 20 Ω and 40 Ω the changes in I_c and BFOR are marginal. These results indicate that, under the present design and test conditions, the footing resistance should be maintained at or below 10 Ω to minimize lightning disturbances due to backflashover. The percentage increase in BFOR for footing resistances in the 20 Ω–40 Ω range relative to 10 Ω is presented in Figure 8.

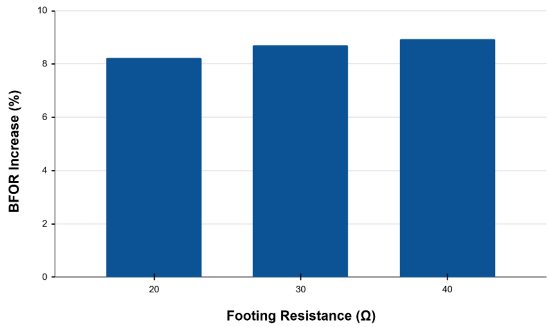

Figure 8. Percentage Increase in Backflashover Rate (BFOR) for Tower Footing Resistances of 20 Ω to 40 Ω Relative to the 10 Ω Baseline

3.0.3 Effect of Arcing Horn Gap Length Variation

Whereas tower footing resistance influences only backflashover, the arcing horn gap length also affects shielding failure performance. Accordingly, the arcing horn gap variation study includes an evaluation of the expected lightning flashover rate (LFR). LFR is defined as the sum of its SFFOR and BFOR [33]:

$$LFR = SFFOR + BFOR \tag{28}$$

As in the preceding analysis, the effect of arcing horn gap length on the critical flashover current is first evaluated. For shielding failure, a 1.3 m gap yields a critical current range of 7 kA to 9.5 kA, when the gap is increased to 1.5 m, the critical current rises to 8 kA to 10.8 kA. For backflashover, a 1.3 m arcing-horn gap yields a critical-current range of 101 kA to 174.4 kA across the tested phase angles. Increasing the gap to 1.5 m raises this range to 119.6 kA–199.9 kA, representing a 15.91% from calculated increase in mean I_c over the 1.3 m reference. Detailed results are presented in Figure 9. Where the upper phase is the phase where backflashover occurs. Besides being influenced by the voltage level from the phase angle, the critical current that causes flashover, I_c, is also influenced by induction from the surrounding phase conductors.

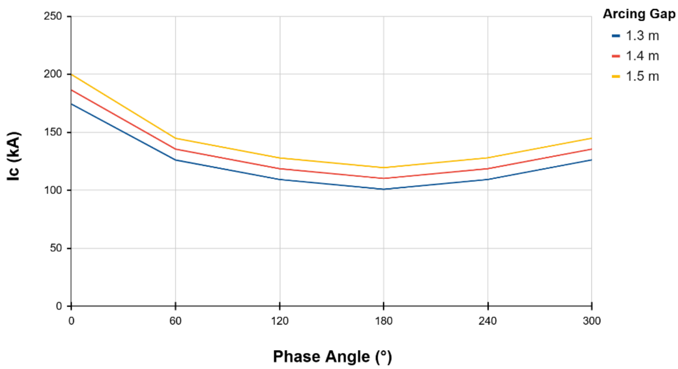

Figure 9. Critical Backflashover Current Range for Shielding Failure Versus Arcing Horn Gap Length

Using the previously determined critical currents, the expected LFR per 100km per year was calculated. For arcing-horn gaps of 1.3 m, 1.4 m, and 1.5 m, the BFORs are 1.666, 1.364, and 1.130 failures per 100 km per year, respectively as presented in Figure 10.

Relative to the 1.3 m baseline, increasing the arcing horn gap to 1.4 m and 1.5 m yields performance gains of up to 13.37 % in SFFOR, 32.13 % in BFOR, and 30.87 % in LFR as presented in Figure 11. However, any adjustment of the arcing horn gap requires a more detailed investigation, owing to the horn's critical function in shielding the insulator from flashover damage. For example, [34] investigates the flashover response of arcing horns and insulators under varied lightning waveform front time and current amplitudes. Although the deviation of critical current that causes flashover from the difference in arcing horn distance is almost linear for each phase angle, due to the lightning distribution probability in equation 19 and the lightning current probability density function in equation 27, this affects the BFOR, SFFOR and LFR values which become non-linear.

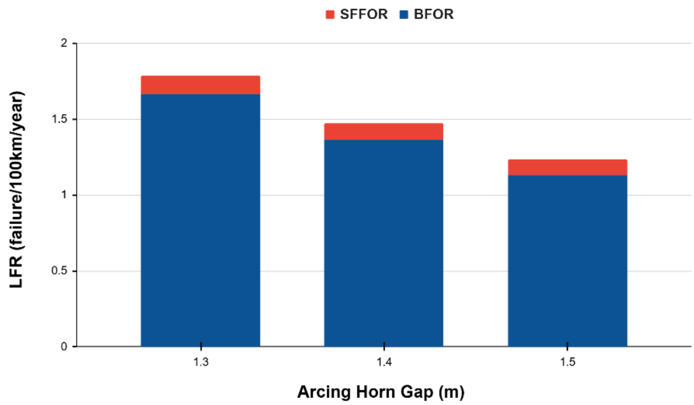

Figure 10. Lightning Flashover Rate (LFR) as a Function of Arcing Horn Gap Length

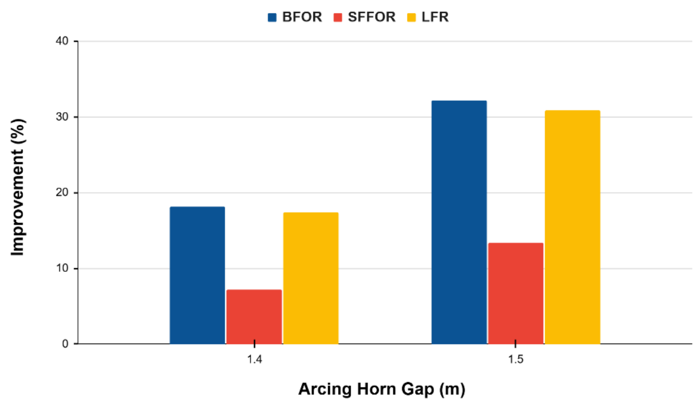

Figure 11. Improvement in BFOR, SFFOR, and LFR for Arcing Horn Gap Lengths of 1.4 m and 1.5 m Relative to the 1.3 m Baseline

4. Conclusion

An exhaustive ATP-EMTP investigation was carried out on a 150 kV lattice type transmission tower representative of PT PLN (Persero) standards to assess its lightning performance under varied model and design parameters. Maximum shielding failure currents were first computed via the EGM using multiple empirical constant sets, yielding interceptable current ranges of 2.53 kA–52.81 kA (median 19.86 kA) across the three phases. Subsequent simulations incorporated a current-dependent footing-resistance model (10 Ω–40 Ω) and three arcing-horn gaps (1.3 m, 1.4 m, 1.5 m), accounting for six system voltage phase angles. Results show that raising footing resistance from 10 Ω to 20 Ω increases BFOR by 8.24 %, with negligible additional impact beyond 20 Ω, while enlarging the horn gap to 1.4 m and 1.5 m reduces LFR by 17.37 % and 30.87 %, respectively, relative to the 1.3 m baseline.

Based on these findings, it is recommended to maintain tower footing resistance at or below 10 Ω and to consider adopting a 1.5 m arcing horn gap with detail investigation, recognizing its critical role in protecting the insulator from flashover damage. Future work should include a detailed evaluation of individual modeling components such as tower footing resistance models, tower surge impedance formulations, and arcing horn flashover algorithms by comparing and correlating simulated predictions with field measurement data. Development of refined analytical or empirical expressions that more accurately reproduce observed lightning strike phenomena is also recommended, as is benchmarking existing ATP-EMTP based studies against on site performance records. Finally, advanced research should explore the design and validation of lightning protection schemes that optimize both effectiveness and cost efficiency.

Acknowledgement

The first author would like to express his deepest gratitude to PT PLN (Persero) for sponsoring this research, in collaboration with the Department of Electrical Engineering, Faculty of Engineering, Universitas Indonesia.

References

[1] S. Hidayat. "Characteristics of lightning discharges in Indonesia". In: *2012 IEEE International Conference on Condition Monitoring and Diagnosis*. IEEE, 2012, pp. 176–179.

[2] L. Colqui et al. "The Impact of Transmission Line Modeling on Lightning Overvoltage". In: *Energies* 16.3 (2023), pp. 1–19.

[3] E. Stracqualursi et al. "Tower Models for Power Systems Transients: A Review". In: *Energies* 15.13 (2022), pp. 1–40.

[4] P. N. Mikropoulos and T. E. Tsovilis. "Lightning attachment models and maximum shielding failure current: Application to transmission lines". In: *2009 IEEE Bucharest PowerTech*. 2009.

[5] N. Zawani et al. "Modelling of 132kV Overhead Transmission Lines by using ATP/EMTP For Shielding Failure Pattern Recognition". In: *Procedia Engineering* 53 (2013), pp. 278–287.

[6] J. Sardi and J. O. C. Chian. "Evaluation of surge arrester requirement for overhead transmission line using electromagnetic transient program". In: *PECon2010 - 2010 IEEE International Conference on Power and Energy*. Kuala Lumpur, Malaysia: IEEE, 2010, pp. 985–988.

[7] N. A. M. Rivas. "Contribution to insulation coordination studies for VSC-HVDC systems". PhD thesis. Université Grenoble Alpes, 2020.

[8] CIGRE Working Group 33.01. *Guide to procedures for estimating lightning performance of transmission lines*. Technical Brochure 063. CIGRE, 1991.

[9] Z. G. Datsios, P. N. Mikropoulos, and T. E. Tsovilis. "Effects of lightning channel equivalent impedance on lightning performance of overhead transmission lines". In: *IEEE Transactions on Electromagnetic Compatibility* 61.3 (2019), pp. 623–630.

[10] M. Ishii et al. "Multistory transmission tower model for lightning surge analysis". In: *IEEE Transactions on Power Delivery* 6.3 (1991), pp. 1327–1335.

[11] CIGRE Working Group C4.23. *Procedures for estimating the lightning performance of transmission lines – New aspects*. Technical Brochure 839. CIGRE, 2021.

[12] EPRI. *AC Transmission Line Reference Book – 200 kV and Above*. Third Edition. Palo Alto, CA: EPRI, 2005.

[13] W. A. Chisholm, Y. L. Chow, and K. D. Srivastava. "Lightning surge response of transmission towers". In: *IEEE Transactions on Power Apparatus and Systems* PAS-102.9 (1983), pp. 3232–3242.

[14] A. Ametani and T. Kawamura. “A method of a lightning surge analysis recommended in Japan using EMTP”. In: *IEEE Transactions on Power Delivery* 20.2 (2005), pp. 867–875.

[15] J. Marti. “Accurate modelling of frequency-dependent transmission lines in electromagnetic transient simulations”. In: *IEEE Transactions on Power Apparatus and Systems* PAS-101.1 (Jan. 1982), pp. 147–157.

[16] J. Hu, H. Li, and Z. Pan. “Study on lightning flashover risk assessment and lightning protection measures of a 220kV”. In: *2022 IEEE International Conference on High Voltage Engineering and Applications (ICHVE)*. Chongqing, China, 2022.

[17] T. Yu and J. Marti. “zCable model for frequency dependent modelling of cable transmission systems”. In: *Proceedings of the International Conference on Power Systems Transients (IPST)*. 2001.

[18] R. A. R. Moura et al. “Influence of the soil and frequency effects to evaluate atmospheric overvoltages in overhead transmission lines - Part I: The influence of the soil in the transmission lines parameters”. In: *International Conference on Atmospheric Electricity (ICAE)*. June. 2014, pp. 15–20.

[19] Z. G. Datsios, P. N. Mikropoulos, and T. E. Tsovilis. “Insulator string flashover modeling with the aid of an ATPDraw object”. In: *2011 46th International Universities Power Engineering Conference (UPEC)*. 2011.

[20] R. Zoro. “Tropical lightning current parameters and protection of transmission lines”. In: *International Journal of Electrical Engineering and Informatics* 11.3 (2019), pp. 506–514.

[21] IEEE Standard. *IEEE guide for improving the lightning performance of transmission lines*. IEEE Std 12431997. 1997.

[22] CIGRE Working Group C4.26. *Evaluation of lightning shielding analysis methods for EHV and UHV DC and AC transmission lines*. Technical Brochure 704. CIGRE, 2017.

[23] K. D. Mousa and A. M. Srivastava. “A revised electrogeometric model for the termination of lightning strokes on ground objects”. In: *Proceedings of the International Aerospace and Ground Conference on Lightning and Static Electricity*. Oklahoma City, 1988, pp. 342–352.

[24] C. F. Wagner and A. R. Hileman. “The lightning stroke-II”. In: *Transactions of the American Institute of Electrical Engineers, Part III: Power Apparatus and Systems* 80.3 (1961), pp. 622–636.

[25] F. S. Young, J. M. Clayton, and A. R. Hileman. “Shielding of transmission lines”. In: *IEEE Transactions on Power Apparatus and Systems, Special Supplement* S82 (1963), pp. 132–154.

[26] H. R. Armstrong and E. R. Whitehead. “Field and Analytical Studies of Transmission Line Shielding”. In: *IEEE Transactions on Power Apparatus and Systems* 87.1 (1968), pp. 270–281.

[27] G. W. Brown and E. R. Whitehead. “Field and analytical studies of transmission line shielding: part II”. In: *IEEE Transactions on Power Apparatus and Systems* PAS-88.No (1969), pp. 617–626.

[28] Earl Ronald Love. “Improvements in lightning stroke modeling and applications to design of EHV and UHV transmission lines”. PhD thesis. University of Colorado, 1973.

[29] E. R. Whitehead. “CIGRE survey of the lightning performance of EHV transmission lines”. In: 1974, pp. 63–89.

[30] R. H. Golde. “The frequency of occurrence and the distribution of lightning flashes to transmission lines”. In: *Electrical Engineering* 64.12 (2013), pp. 902–910.

[31] J. G. Anderson. *Transmission Line Reference Book-345 kV and above*. 2nd. Palo Alto, CA: Electric Power Research Institute, 1982. Chap. 12.

[32] P. N. Mikropoulos and T. E. Tsovilis. “Estimation of the shielding performance of overhead transmission lines: The effects of lightning attachment model and lightning crest current distribution”. In: *IEEE Transactions on Dielectrics and Electrical Insulation* 19.6 (2012), pp. 2155–2164.

[33] Z. G. Datsios et al. “Application of non-gapped line surge arresters to the 150 kV overhead lines of Rhodes: an investigation through ATP-EMTP simulations”. In: *2021 35th International Conference on Lightning Protection (ICLP 2021) and 16th International Symposium on Lightning Protection (SIPDA 2021)*. Sri Lanka, 2021.

[34] W. Naon and S. Premrudeepreechacharn. “Flashover Occurrence Factor of Insulator String with Arc Horn on High Voltage Transmission Line”. In: *41st North American Power Symposium (NAPS 2009)*. 2009, pp. 1–5.